

Submitted to Materials Science and Engineering: A

Crack-healing behavior of Si₃N₄/SiC composite under stress and low oxygen pressure

Koji Takahashi ^a, Young-Soon Jung ^a, Yasuto Nagoshi ^a, Kotoji Ando ^a

^a Department of Materials Engineering, Yokohama National University, 79-5, Tokiwadai, Hodogaya-ku, Yokohama, 240-8501, Japan

Correspondence:

Dr. Koji Takahashi
Faculty of Engineering,
Yokohama National University,
79-5, Tokiwadai, Hodogaya, Yokohama, 240-8501, Japan.
E-mail: ktaka@ynu.ac.jp
TEL: 81-45-339-4017
FAX 81-45-339-4024

Abstract

The crack-healing behavior of Si₃N₄/SiC composite under constant stress and low oxygen partial pressure was investigated. A semi-elliptical surface crack with a length of about 100 μm was introduced at the center of the tensile surface by the indentation method. The specimens were crack-healed at 1200°C for 5 h under tensile stress ($\sigma_{app.}=200-300$ MPa) and under low oxygen partial pressure and air ($P_{O_2}=50-21000$ Pa). The threshold constant stress for crack-healing was defined as 200 MPa in oxygen partial pressure over 500 Pa. The bending strengths of crack-healed specimens under tensile stress in $P_{O_2}\geq 500$ Pa showed almost the same value as a healed smooth specimen, and most specimens fractured outside the crack-healed zone. From these results, we conclude that crack-healing can be achieved under stress in low oxygen pressure and can lengthen lifetime and increase reliability in Si₃N₄/ SiC composite ceramic.

Key words: *Si₃N₄/ SiC, Crack-healing, Low oxygen partial pressure, In situ observation*

1. Introduction

Some structural ceramics have a self-crack-healing ability [1-10]. If this ability is used on ceramic components, great merits can be anticipated in the following areas: (a) an increase in reliability [11, 12], (b) decreases in inspection, machining and polishing costs [13,14], and (c) decreases in maintenance costs and prolongation of the lifetime of the ceramic [15-17].

However, if a crack is initiated during service, the reliability of the ceramic will be considerably reduced because the fracture toughness of structural ceramics is not high. If a crack can be healed under service conditions, e.g., under tensile stress and at high temperatures, the reliability and lifetime of the ceramic components for high temperature applications such as micro gas turbine blades can be increased. The crack-healing behavior of Si₃N₄/SiC under stress at 800 - 1000°C in air was investigated [16]. It was found that a surface crack of 100 μm could be healed completely even under constant or cyclic stress at 800 - 1000°C [16]. Also, it was reported that a surface crack of 100 μm could be healed completely in just 0.5-1 h even under cyclic stress at 1100 and 1200°C in air [17]. These results indicate that Si₃N₄/SiC has excellent crack-healing ability.

Crack-healing can be achieved by the oxidation of Si₃N₄ and SiC in Si₃N₄/SiC composite. However, the gas turbine blades and engine components are commonly used in combustion

environments, which have lower oxygen partial pressure than the air atmosphere [18]. Most studies on the self-crack-healing of ceramics up to now have been conducted in air. Recently, the self-crack-healing behaviors of Si₃N₄/SiC [19] and Al₂O₃/SiC [20] composites under low oxygen-partial-pressure conditions have been reported.

However, the crack-healing behavior under stress in low oxygen-partial-pressure conditions has not yet been studied. In this paper, the crack-healing behavior of Si₃N₄/SiC under constant tensile stress in low oxygen-partial-pressure conditions and in air was investigated at 1200°C. In situ observations of crack-healing were also carried out to investigate the crack-healing behavior.

2. Experimental Procedure

2.1 Material and specimens

The silicon nitride powder (SN-E10, Ube Industries Ltd., Ube, Japan) used in this study has a mean particle size of 0.2 μm; the volume ratio of α-Si₃N₄ is about 95%, with the rest being β-Si₃N₄. The SiC powder (Ultrafine grade, Ibiden Co. Ltd., Ogaki, Japan) used has a 0.27-μm mean particle size. The samples were prepared using a mixture of silicon nitride with 20 wt% SiC powder and 8 wt% Y₂O₃ as a sintering additive powder. The Y₂O₃ powder (Fine grade, Nippon Yttrium Co. Ltd., Oomuta, Japan) used has a 0.4-μm mean particle size. To this mixture, alcohol was added and blended completely for 48 h. The mixture was placed in an evaporator to extract the solvent and then in a vacuum to produce a dry powder mixture. The mixture was subsequently hot-pressed at 1850°C and 35 MPa for 2 h in an N₂ atmosphere. The relative density of the hot-pressed material determined by the Archimedes method was 99.5 % of the theoretical density (3.32 kgf/mm³). The average grain size of the matrix was Si₃N₄=0.44 μm, and the average aspect ratio was about 5.0. Figure 1 shows the XRD pattern of the as-received specimen. The grain boundary phases were Y₂₀N₄Si₁₂O₄₈ and YSiO₂N. Most SiC particles were located in grain boundaries and distributed uniformly. This silicon nitride was selected as a test material because it has an excellent crack-healing ability. The sintered plate was then cut into test specimens measuring 2×4×40 mm. The specimens were polished to a mirror finish on one face.

Semi-elliptical surface cracks of 100 μm in surface length were introduced at the center of the tensile surface of the specimens using a Vickers indenter at a load of 19.6 N. The ratio of depth (*a*) to half the surface length (*c*) of the crack (aspect ratio) was $a/c \doteq 0.9$.

2.2 Experimental method

In this study, crack-healing was carried out under constant bending stress using an in-situ observation apparatus. Figure 2 shows a schematic illustration of the in-situ observation apparatus used in this study. This apparatus consisted of an infrared image furnace, a 3-point bending device and an optical microscope with a CCD camera. The maximum temperature and the maximum load of the system were 1200 °C and 500 N, respectively. The pre-cracked specimens were crack-healed under constant bending stress ($\sigma_{app.}=200, 250$ and 300 MPa) at 1200°C in various oxygen partial pressure conditions ($P_{O_2}= 50, 500$ and 5000 Pa) and in air ($P_{O_2}= 21000$ Pa). A N_2 - O_2 gas mixture flowed into the heat system during the crack-healing process. The oxygen partial pressure of 50, 500 and 5000 Pa was controlled by passing N_2 impurely O_2 of 500 ppm, N_2 -0.50% O_2 , and N_2 -5.00% O_2 , respectively. After the temperature was increased to 1200°C, constant bending stress was applied by three-point bending with a span length of 26 mm, as shown in Fig. 2. The motion pictures taken during the crack-healing process were observed in situ by optical microscopy, and were recorded to computer with a CCD camera.

After the crack-healing process, the bending strengths of the specimens were measured at room temperature in air. Normally, three specimens were used to establish the monotonic bending strength. These tests were carried out using a universal monotonic testing machine. The cross-head speed for the monotonic bending tests was 0.5 mm/min.

3. Results and discussion

3.1 Crack-healing condition

Figure 3 shows the relationship between the bending strength at room temperature and the crack-healing time at 1200°C under a tensile stress ($\sigma_{app.}$) of 200 MPa in $P_{O_2}=500$ Pa. The applied stress of 200 MPa was 45% of the bending strength of the pre-cracked specimens. The solid circles indicate the bending strength (σ_B) of the smooth specimen healed at 1300°C for 1 h in air. The open triangles indicate the bending strength of the pre-cracked specimens. The average bending strength of the smooth specimens was 930 MPa, and that of the pre-cracked specimens was 440 MPa. The bending strength of the pre-cracked specimens decreased by 53% due to the pre-cracks introduced by the Vickers indentation.

The solid square symbols indicate the bending strengths of the crack-healed specimens which crack-healed at 1200°C under a stress of 200 MPa in $P_{O_2}=500$ Pa. In the specimens with asterisks, fracturing occurred outside of the crack-healed zone as shown in Fig.4, which indicated that the pre-crack was healed completely. For the 1 h crack-healing treatment, the bending strengths increased up to about 720 MPa, but this did not represent complete strength

recovery. On the other hand, for the 5 h crack-healing treatment, the crack-healed specimens significantly recovered their strength, to a value of about 850 MPa. By means of the crack-healing at 1200°C for 5 h, the crack-healed specimen showed almost the same strength as the healed smooth specimen. Moreover, the fracturing in two specimens occurred outside the crack-healed zone. Therefore, it was confirmed that complete strength recovery could be achieved under tensile stress in low oxygen-partial-pressure conditions ($\sigma_{app.}=200$ MPa, $P_{O_2}=500$ Pa) by crack-healing at 1200°C for 5 h.

3.2 Threshold stress for crack-healing under service conditions

Figures 5 (a), (b), (c) and (d) show the results of bending tests on specimens crack-healed under constant stress in $P_{O_2}=21000$, 5000, 500 and 50 Pa, respectively. The solid symbols represent the bending strengths of the specimens crack-healed at a healing temperature of 1200°C for 5 h. Open triangle symbols indicate the bending strengths of the pre-cracked specimens. The asterisks indicate specimens that fractured outside the crack-healed zone, suggesting that the pre-cracks were healed completely. The threshold stresses for crack-healing were defined as the maximum stresses below which the crack-healed specimens recovered their bending strengths and below which most the specimens fractured outside the crack-healed zone.

In the case of crack-healing in air ($P_{O_2}=21000$ Pa), as shown in Fig. 5 (a), the specimens crack-healed under a constant stress of 200 MPa showed quite high bending strength, comparable to that of the specimens crack-healed under no stress. Most of the specimens crack-healed under 200 MPa fractured outside the crack-healed zone. However, the specimens crack-healed under a constant stress of 250 MPa showed low bending strength and fractured in the crack-healed zone. Therefore, the threshold stress for crack-healing in air was determined to be 200 MPa.

By the same method, the threshold stresses for crack-healing in $P_{O_2}=5000$ and 500 Pa, were determined to be 200 MPa in both cases, as shown in Figs. 5 (b) and (c), respectively. These results indicate that complete strength recovery could be achieved by crack-healing even under service conditions, i.e., with an applied stress below $\sigma_{app.}=200$ MPa and an oxygen partial pressure over $P_{O_2}=500$ Pa.

The specimens crack-healed in $P_{O_2}=50$ Pa did not fracture during the crack-healing process under 200 MPa or 250 MPa, but the bending strength did not recover completely, as shown in Fig.5 (d). All specimens fractured from crack-healed zone. Thus, the threshold stress for crack-healing could not be determined in $P_{O_2}=50$ Pa. A strength recovery of about 200 MPa could be obtained by releasing the tensile residual stress, which was introduced by the

indentation method. In the previous study, it was reported that the optimized crack-healing conditions in $P_{O_2}=50$ Pa were a temperature of 1300°C and a time of 10 h [19]. Therefore, the healing condition of 1200°C for 5 h was insufficient for the formation of oxidation products to completely bond the crack wall.

3.3 In-situ observation of crack-healing under stress

Figure 6 (a) shows images taken during the crack-healing process at 1200°C under 200 MPa tensile stress in $P_{O_2}=50$ Pa. The length of the pre-crack was about 100 μm . At 0 h, the pre-cracks could be clearly observed. Then, slow crack growth was observed in a direction perpendicular to the tensile stress in $P_{O_2}=50$ Pa. The cracks propagated, but the specimen was not fractured during the crack-healing process. Cracks were clearly observed after 5 h. For this reason, complete strength recovery could not be achieved under this crack-healing condition.

Figure 6 (b) shows images taken during the crack-healing process at 1200°C under 200 MPa tensile stress in air ($P_{O_2}=21000$ Pa). The pre-cracks could barely be observed after 3 h in $P_{O_2}=21000$ Pa because the surface was covered with oxidation products such as SiO_2 and $\text{Y}_2\text{Si}_2\text{O}_7$ [13, 17, 21]. These sufficient oxidation products cover the crack surface and bond the crack wall through heat generation and volume expansion [9, 22]. Thus, complete strength recovery could be achieved under this crack-healing condition. For specimens crack-healed under 200 MPa in $P_{O_2}=500$ and 5000 Pa, the crack-healing behavior was similar to that in the case of $P_{O_2}=21000$ Pa.

Figure 7 shows images taken during the crack-healing process at 1200°C under 250 MPa tensile stress in air ($P_{O_2}=21000$ Pa). The cracks emanated at the initial crack tips and propagated after 3 h. The cracks did not propagate after 5 h. For specimens crack-healed under 250 MPa in $P_{O_2}=500$ and 5000 Pa, the crack-healing behavior was similar to that in the case of $P_{O_2}=21000$ Pa. The cracks were not completely healed as shown in Fig. 7. For this reason, complete strength recovery could not be achieved as mentioned in the previous section.

3.4 Relationship between the oxidized layer thickness and oxidation partial pressure

The oxidized layer thicknesses were analyzed based on fracture surface observation using SEM, after crack-healing at 1200°C for 5h, as a function of oxygen partial pressure. Figure 8 shows the relationship between the oxidation partial pressure and the oxidized layer thickness. The oxidized layer thickness of the crack-healed specimens in $P_{O_2}=50$ Pa was about 0.3 μm . This indicates that the oxidation reactions occurred in the surface area, but were not sufficient to heal the cracks. The crack opening size was about 0.2-0.3 μm , and the depth was about 40~50

μm . Therefore, greater heat generation at a higher temperature or for a longer time would be required to heal the crack completely.

On the other hand, the oxidized layer thickness was significantly increased by crack-healing in $P_{\text{O}_2} \geq 500$ Pa. The thickness was about $1.7 \mu\text{m}$. By means of the formation of an oxidation layer, the cracks were completely filled with oxidation products, and the strengths were completely recovered.

4. Conclusions

The crack-healing behavior of $\text{Si}_3\text{N}_4/\text{SiC}$ composite under constant stress and low oxygen partial pressure was investigated. The specimens having pre-cracks of $100 \mu\text{m}$ in surface length were crack-healed at 1200°C for 5 h under tensile stress of $\sigma_{\text{app.}}=200\text{-}300$ MPa and under oxygen partial pressure of $P_{\text{O}_2}=50, 500, 5000, 21000$ Pa. The results were summarized as follows:

- (1) In $P_{\text{O}_2} \geq 500$ Pa, the threshold constant stresses for crack-healing were defined as 200 MPa. These threshold stresses were 45% of the bending stress of the pre-cracked specimens (~ 440 MPa). Thus, pre-cracks of $100 \mu\text{m}$ in surface length, which reduced the bending strength by 53%, could be healed completely even under a tensile stress and low oxygen partial pressure.
- (2) In $P_{\text{O}_2}=50$ Pa, the bending strength did not recover completely and all specimens fractured from crack-healed zone. Thus, the threshold stress for crack-healing could not be determined by the crack-healing at 1200°C for 5 h.
- (3) In situ observations of crack-healing in $P_{\text{O}_2} \geq 500$ Pa indicated that cracks were healed under $\sigma_{\text{app.}}=200$ MPa. Thus, complete strength recovery could be achieved under these crack-healing conditions. On the other hand, the crack propagation occurred under $\sigma_{\text{app.}}=250$ MPa and the cracks were not completely healed.
- (4) In situ observations of crack-healing in $P_{\text{O}_2}=50$ Pa indicated that cracks were not healed. Thus, complete strength recovery could not be achieved under these crack-healing condition.
- (5) The oxidized layer thickness was significantly increased by crack-healing in $P_{\text{O}_2} \geq 500$ Pa. By means of the formation of an oxidation layer, the cracks were completely filled with oxidation products, and the strengths were completely recovered.

References

- [1] T. K. Gupta, Crack healing and strengthening of thermally shocked alumina, J. Am Ceram.

Soc., 89[5-6] (1979) 259-262,.

[2] M. Mitomo, T. Nishimura, M. Tsutsumi, Crack healing in silicon nitride and alumina ceramics, *J. Mater. Sci. Lett.*, 15 (1996) 1976-1978.

[3] S. R. Choi, V. Tikare, Crack healing behavior of hot pressed silicon nitride due to oxidation, *Scr. Metall. Mater.*, 26 (1992) 1263-1268.

[4] K. Ando, T. Ikeda, S. Sato, F. Yao, Y. Kobayashi, A preliminary study on crack healing behavior of Si₃N₄/SiC composite ceramics, *Fatigue Fract. Eng. Mater. Struct.*, 21 (1998) 119-122.

[5] Y. H. Zhang, L. Edwards, W. J. Plumbridge, Crack healing in a silicon nitride ceramic, *J. Am. Ceram. Soc.*, 81[7] (1998) 1861-1868.

[6] Y.W. Kim, K. Ando, M.C. Chu, Crack healing behavior of liquid-phase-sintered silicon carbide ceramics, *J. Am. Ceram. Soc.*, 86 (2003) 465–70.

[7] Z. Chlup, P. Flasar, K. Ando, I. Dlouhy, Fracture behaviour of Al₂O₃/SiC nanocomposite ceramics after crack healing treatment, *J. Eur. Ceram. Soc.*, 28 (2008) 1073–1077.

[8] K.W. Nam, M.K. Kim, S.W. Park, S.H. Ahn, J.S. Kim, Crack-healing behavior and bending strength of Si₃N₄/SiC composite ceramics by SiO₂ colloidal, *Mater. Sci. and Engng A* 471 (2007) 102–105.

[9] W. Nakao, K. Takahashi, K. Ando, Self-healing of surface cracks in structural ceramics, in: S.K. Ghosh (Ed.), *Self-Healing Materials: Fundamentals, Design Strategies, and Applications*, WILEY-VCH, Weinheim, 2008, pp. 183-217.

[10] K. Ando, K. Takahashi, W. Nakao, Self-crack-healing behavior of structural ceramics, in: T.Y. Tseng and H.S. Nalwa (Eds.), *Handbook of nanoceramics and their based nanodevice Vol.3*, American Scientific Publishers, California, 2009, pp. 1-26.

[11] K. Ando, M.C. Chu, S. Matsushita, S. Sato, Effect of crack-healing and proof-testing procedures on fatigue strength and reliability of Si₃N₄/SiC composites, *J. Eur. Ceram. Soc.*, 23 (2003) 977-984.

- [12] M. Ono, W. Nakao, K. Takahashi, M. Nakatani, K. Ando, A new methodology to guarantee the structural integrity of Al₂O₃/SiC composite using crack healing and a proof test, *Fatigue Fract. Eng. Mater. Struct.*, 30 (2007) 599-607.
- [13] Y. S. Jung, Y. Guo, W. Nakao, K. Takahashi, K. Ando, S. Saito, Crack-healing behaviour and resultant high-temperature fatigue strength of machined Si₃N₄/SiC composite ceramic, *Fatigue Fract. Eng. Mater. Struct.*, 31 (2008) 2-11.
- [14] T. Osada, W. Nakao, K. Takahashi, K. Ando, S. Saito, Strength recovery behavior of machined Al₂O₃/SiC nano-composite ceramics by crack-healing, *J. Eur. Ceram. Soc.*, 27 (2007) 3261-3267.
- [15] F. Yao, K. Ando, M.C. Chu, S. Sato, Static and cyclic fatigue behavior of crack-healed Si₃N₄/SiC composite ceramics, *J. Eur. Ceram. Soc.*, 21 (2001) 991-997.
- [16] K. Takahashi, B.S. Kim, M.C. Chu, S. Sato, K. Ando, Crack-healing behavior and static fatigue strength of Si₃N₄/SiC ceramics held under stress at temperature (800, 900, 1000 °C), *J. Eur. Ceram. Soc.*, 23 (2003) 1971-1978.
- [17] K. Takahashi, K. Ando, H. Murase, S. Nakayama, S. Saito, Threshold stress for crack-healing of Si₃N₄/SiC and resultant cyclic fatigue strength at the healing temperature, *J. Am. Ceram. Soc.*, 88 (2005) 645-651.
- [18] N.S. Jacobson, Corrosion of silicon-based ceramics in combustion environments, *J. Am. Ceram. Soc.*, 76 (1993) 3-28.
- [19] Y. S. Jung, W. Nakao, K. Takahashi, K. Ando, S. Saito, Crack-healing behavior of Si₃N₄/SiC composite under low oxygen partial pressure, *J. Soc. Mater. Sci. Jpn.*, 57 (2008) 1132-1137.
- [20] T. Osada, W. Nakao, K. Takahashi, K. Ando, Kinetics of self-crack-healing of alumina/silicon carbide composite including oxygen partial pressure effect, *J. Am. Ceram. Soc.*, 92 (2009) 864-869.
- [21] K. Houjou, K. Ando, S. P. Liu, S. Sato, Crack-healing and oxidation behavior of silicon nitride ceramics, *J. Eur. Ceram. Soc.*, 24 (2004) 2329-2338.

[22] F. L. Riley, Silicon nitride and related materials, J. Am. Ceram. Soc., 83 (2000) 245-265.

Captions of figures

Fig.1 XRD profiles of the as-received Si₃N₄/SiC.

Fig.2 Schematic illustration of in-situ observation experimental apparatus.

Fig.3 Relationship between bending strength at room temperature and crack-healing time at 1200 °C under tensile stress of 200 MPa in $P_{O_2}=500$ Pa.

Fig.4 Fracture patterns of crack-healed Si₃N₄/SiC. (a) Fracture surface, (b) Specimen surface, Fracture occurred outside the crack-healed zone. (Healing condition: 1200 °C for 5 h, $P_{O_2}=500$ Pa, $\sigma_{app} = 200$ MPa)

Fig.5 Bending strengths of crack-headlined specimens as a function of applied stress during crack-healing in (a) air ($P_{O_2} = 21000$ Pa), (b) $P_{O_2} = 5000$ Pa, (c) $P_{O_2} = 500$ Pa, and (d) $P_{O_2} = 50$ Pa.

Fig.6 In-situ observation image during crack-healing process at 1200 °C for 5 h under 200 MPa in (a) $P_{O_2}=50$ Pa and (b) air ($P_{O_2}=21000$ Pa). Arrows indicate crack tip.

Fig.7 In-situ observation image during crack-healing process at 1200 °C for 5 h under 250 MPa in air ($P_{O_2}=21000$ Pa). Arrows indicate crack tip.

Fig.8 Relationship between oxidation layer thickness and oxygen partial pressure.

Captions of figures

Fig.1 XRD profiles of the as-received $\text{Si}_3\text{N}_4/\text{SiC}$.

Fig.2 Schematic illustration of in-situ observation experimental apparatus.

Fig.3 Relationship between bending strength at room temperature and crack-healing time at 1200°C under tensile stress of 200 MPa in $P_{\text{O}_2}=500$ Pa.

Fig.4 Fracture patterns of crack-healed $\text{Si}_3\text{N}_4/\text{SiC}$. (a) Fracture surface, (b) Specimen surface, Fracture occurred outside the crack-healed zone. (Healing condition: 1200°C for 5 h, $P_{\text{O}_2}=500\text{Pa}$, $\sigma_{\text{app}}=200\text{MPa}$)

Fig.5 Bending strengths of crack-headlined specimens as a function of applied stress during crack-healing in (a) air ($P_{\text{O}_2}=21000$ Pa), (b) $P_{\text{O}_2}=5000$ Pa, (c) $P_{\text{O}_2}=500$ Pa, and (d) $P_{\text{O}_2}=50$ Pa.

Fig.6 In-situ observation image during crack-healing process at 1200°C for 5 h under 200 MPa in (a) $P_{\text{O}_2}=50$ Pa and (b) air ($P_{\text{O}_2}=21000$ Pa). Arrows indicate crack tip.

Fig.7 In-situ observation image during crack-healing process at 1200°C for 5 h under 250 MPa in air ($P_{\text{O}_2}=21000$ Pa). Arrows indicate crack tip.

Fig.8 Relationship between oxidation layer thickness and oxygen partial pressure.

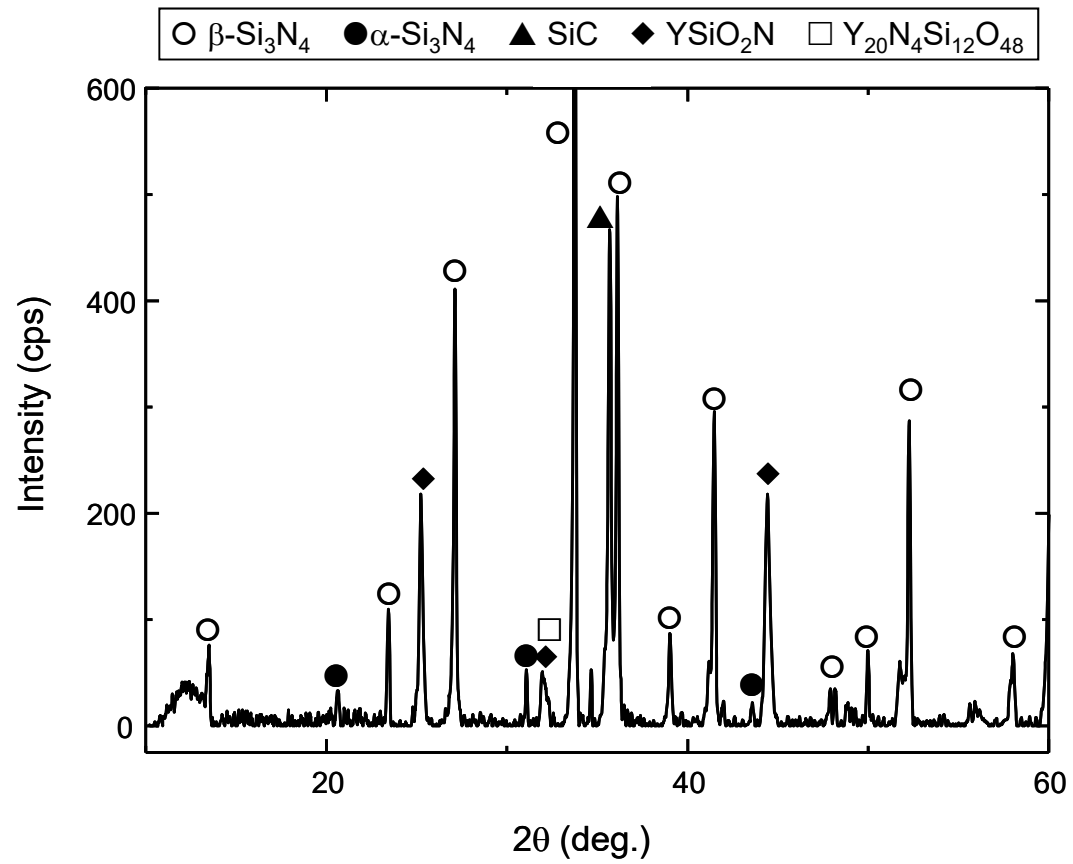


Fig. 1 XRD profiles of the as-received Si₃N₄/SiC.

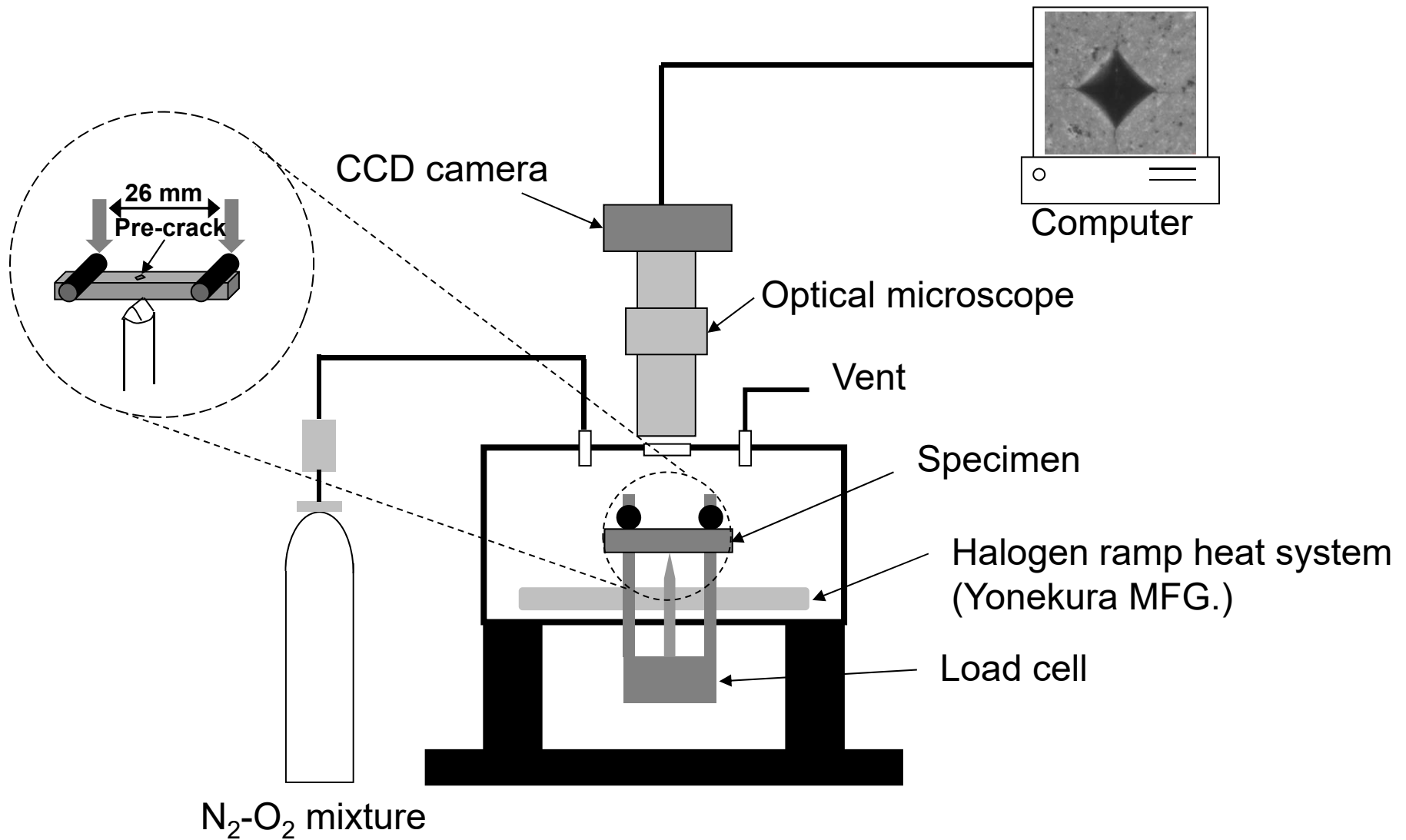


Fig. 2 Schematic illustration of in-situ observation experimental apparatus.

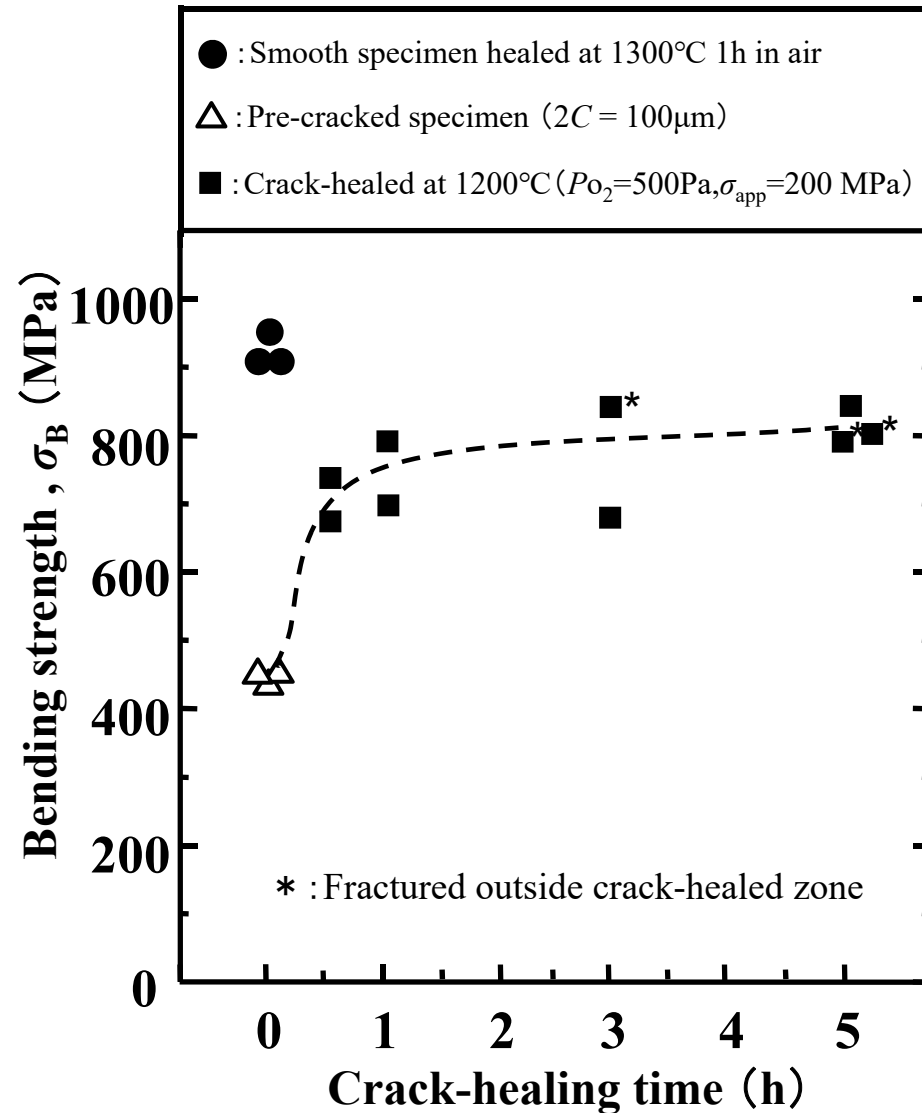
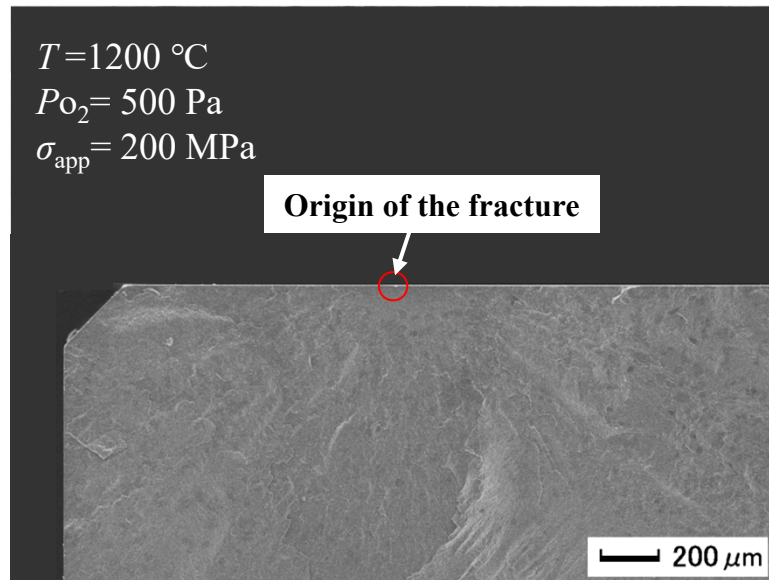
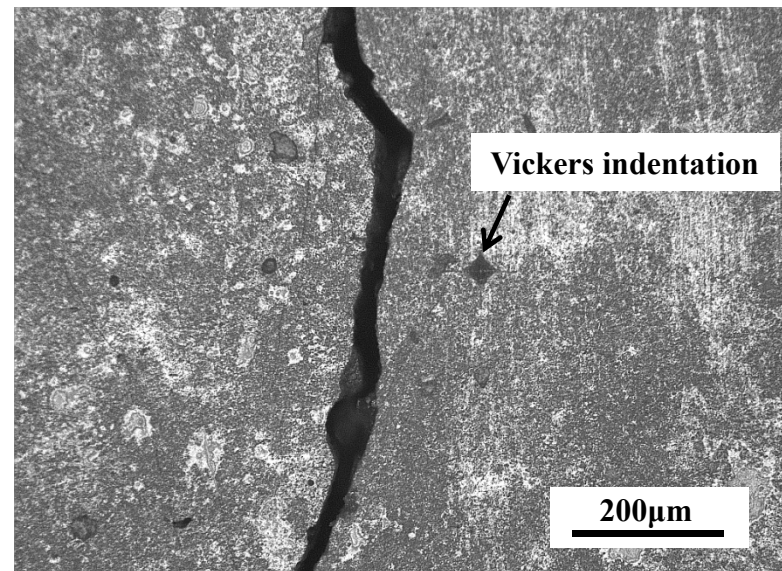


Fig.3 Relationship between bending strength at room temperature and crack-healing time at 1200°C under tensile stress of 200 MPa in $P_{\text{O}_2}=500\text{ Pa}$.

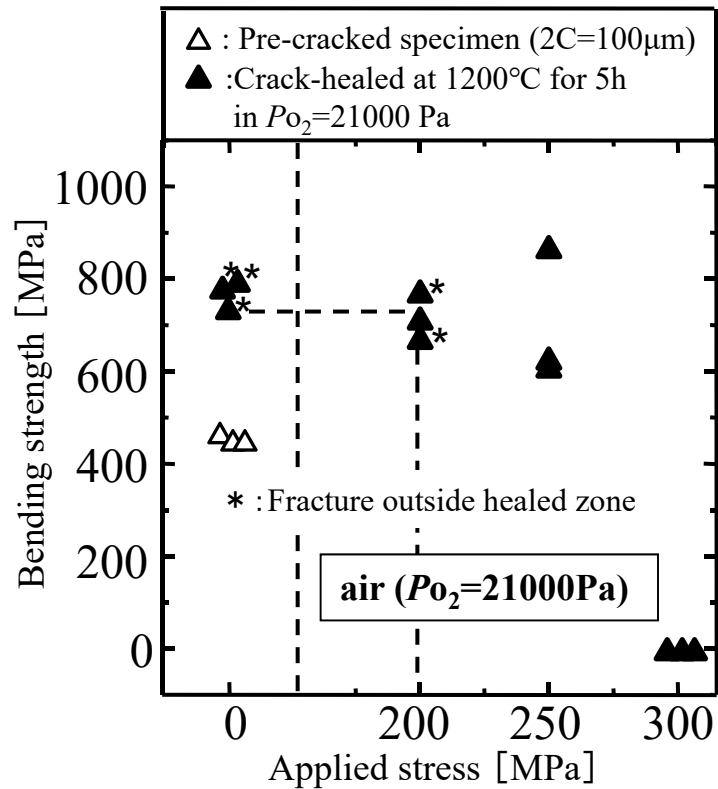


(a) Fracture surface

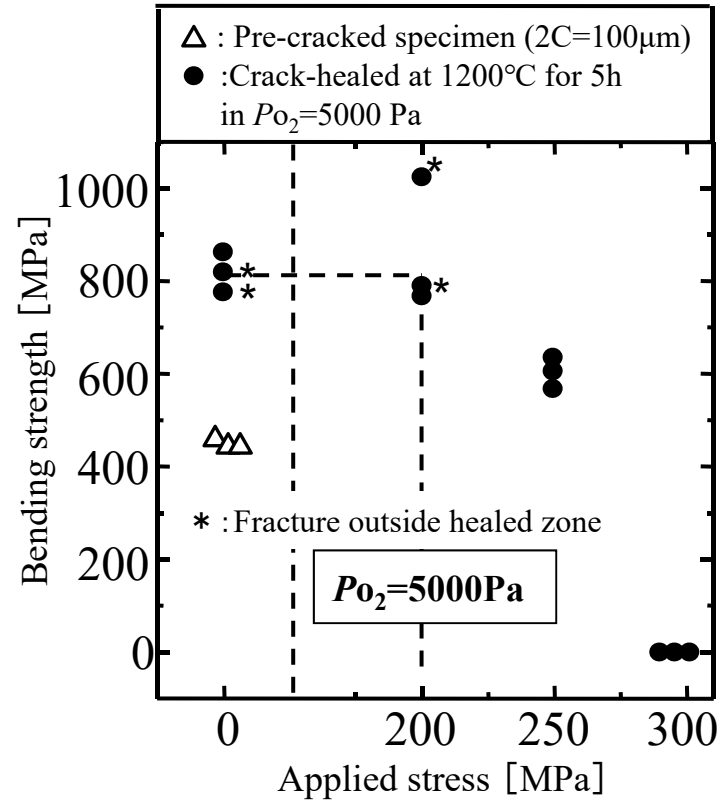


(b) Specimen surface

Fig.4 Fracture patterns of crack-healed $\text{Si}_3\text{N}_4/\text{SiC}$. (a) Fracture surface, (b) Specimen surface, Fracture occurred outside the crack-healed zone. (Healing condition: $1200\text{ }^{\circ}\text{C}$ for 5 h, $P_{\text{O}_2}=500\text{ Pa}$, $\sigma_{\text{app}}=200\text{ MPa}$)

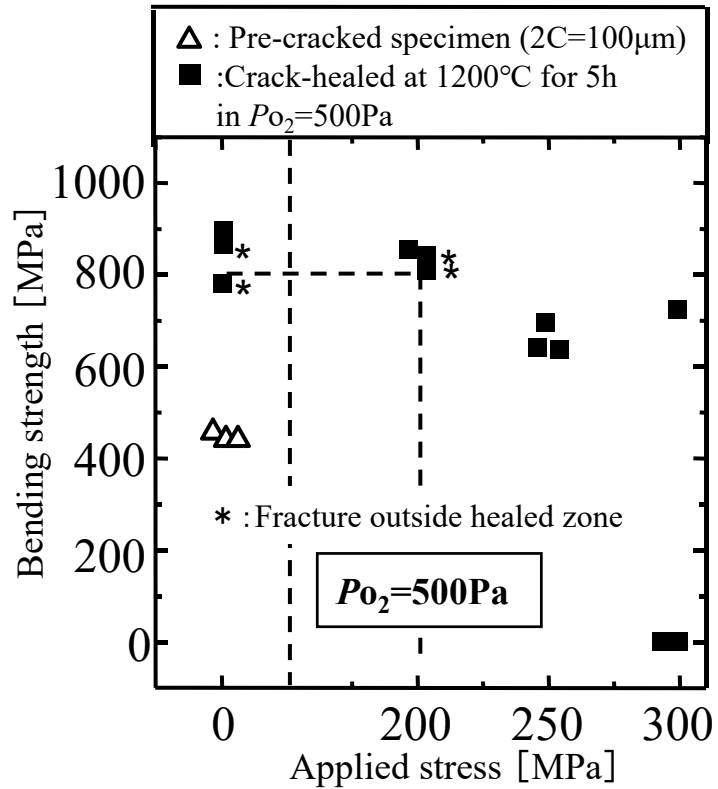


(a) air ($P_{\text{O}_2} = 21000\text{ Pa}$)

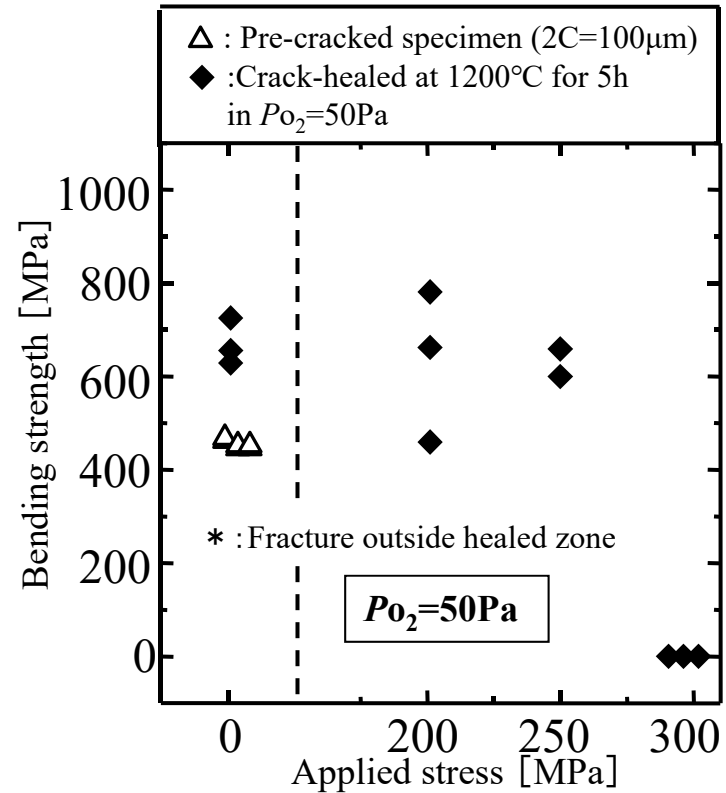


(b) $P_{\text{O}_2} = 5000\text{ Pa}$

Fig.5 Bending strengths of crack-headlined specimens as a function of applied stress during crack-healing in (a) air ($P_{\text{O}_2} = 21000\text{ Pa}$), (b) $P_{\text{O}_2} = 5000\text{ Pa}$, (c) $P_{\text{O}_2} = 500\text{ Pa}$, and (d) $P_{\text{O}_2} = 50\text{ Pa}$.

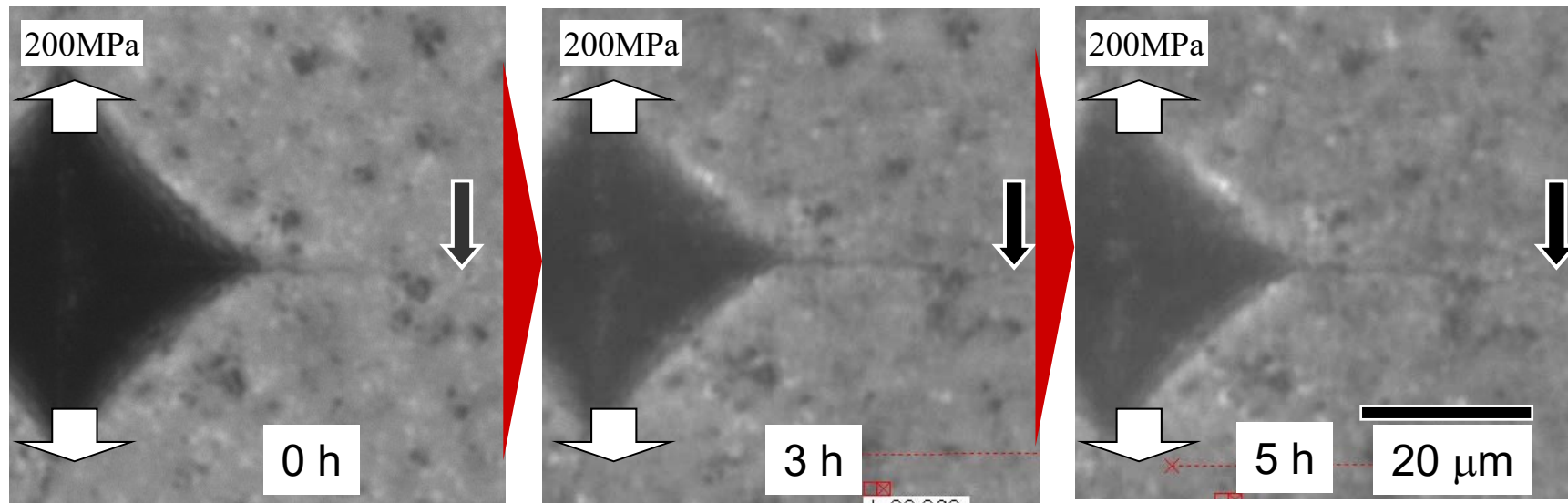


(c) $P_{O_2} = 500 \text{ Pa}$

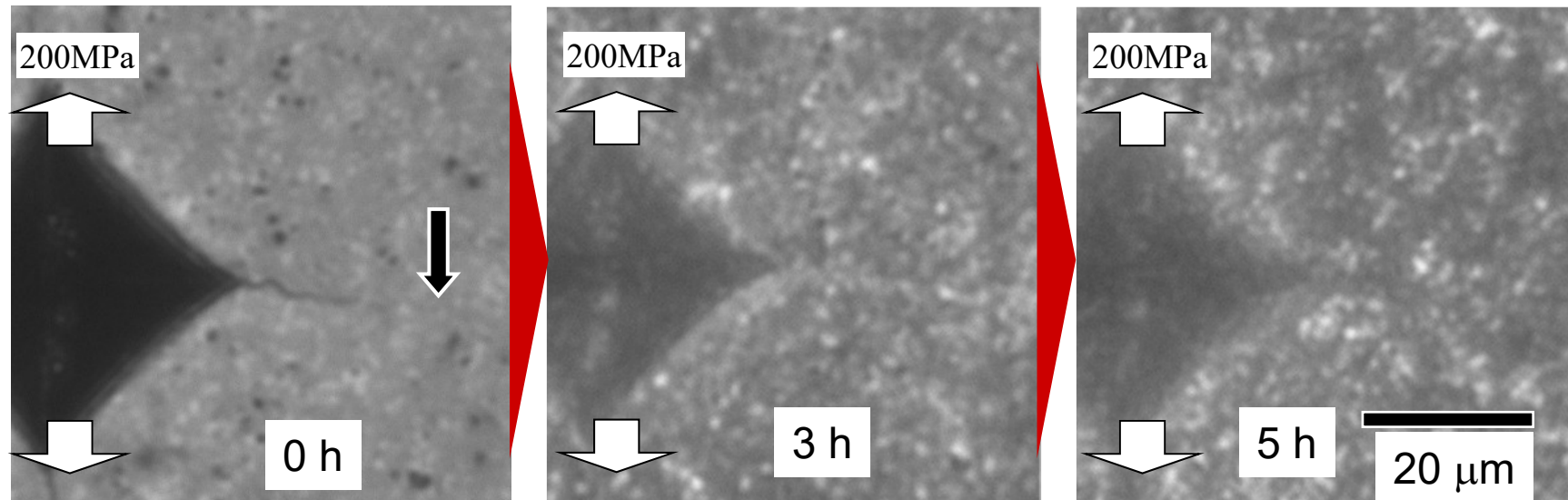


(d) $P_{O_2} = 50 \text{ Pa}$

Fig.5 Bending strengths of crack-headlined specimens as a function of applied stress during crack-healing in (a) air ($P_{O_2} = 21000 \text{ Pa}$), (b) $P_{O_2} = 5000 \text{ Pa}$, (c) $P_{O_2} = 500 \text{ Pa}$, and (d) $P_{O_2} = 50 \text{ Pa}$.



(a) $P_{O_2}=50$ Pa



(b) air ($P_{O_2}=21000$ Pa)

Fig.6 In-situ observation image during crack-healing process at 1200°C for 5 h under 200 MPa in (a) $P_{O_2}=50$ Pa and (b) air ($P_{O_2}=21000$ Pa). Arrows indicate crack tip.

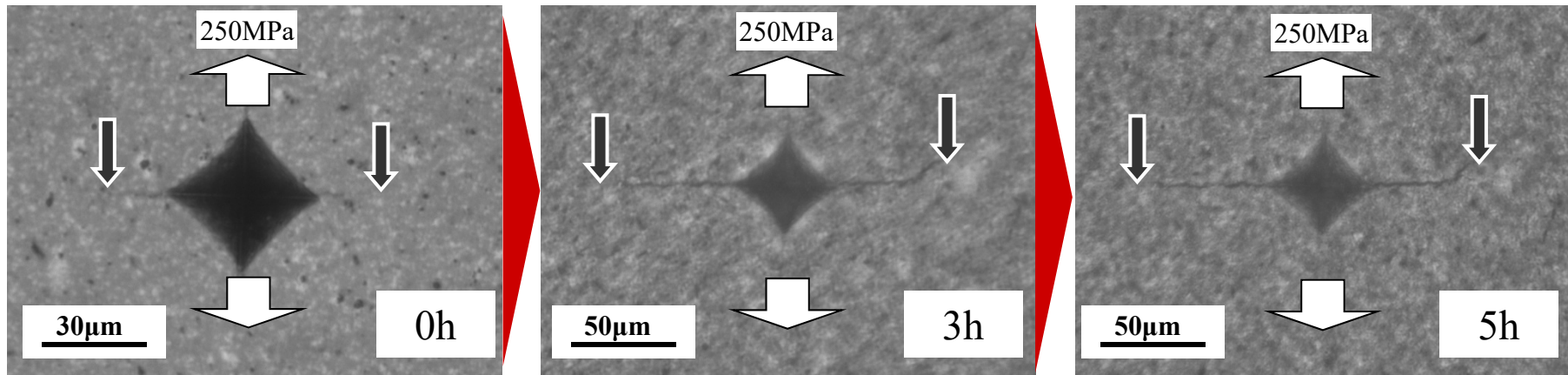


Fig.7 In-situ observation image during crack-healing process at 1200°C for 5 h under 250 MPa in air ($P_{O_2}=21000$ Pa). Arrows indicate crack tip.

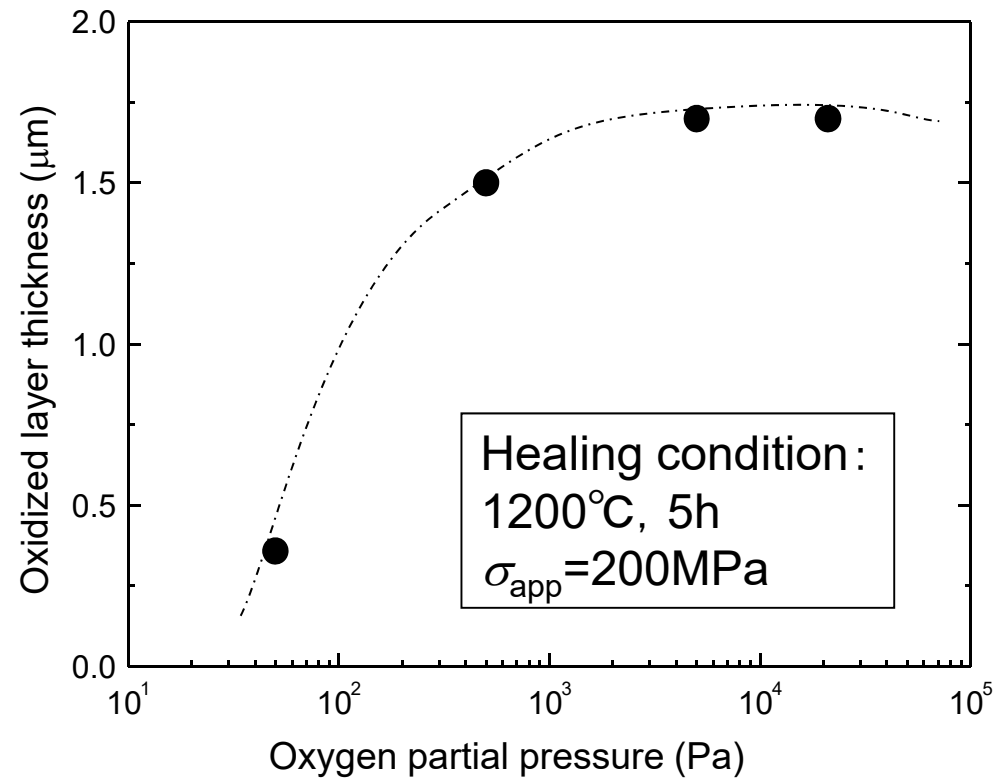


Fig. 8 Relationship between oxidation layer thickness and oxygen partial pressure.